Re-evaluation of Leonian and Liberian events in the geodynamical evolution of the Man-Leo Shield (West African Craton)

Gnagnon Raymond-Stéphane Koffi, Alain Nicaise Kouamelan, Marc Ephrem Allialy, Yacouba M. Coulibaly, Jean-Jacques Peucat

Journal Pre-proofs

Re-evaluation of Leonian and Liberian events in the geodynamical evolution of the Man-Leo Shield (West African Craton)

Gnagnon Raymond-Stéphane Koffi, Alain Nicaise Kouamelan, Marc Ephrem Allialy, Yacouba Coulibaly, Jean-Jacques Peucat

PII: S0301-9268(19)30104-4
DOI: https://doi.org/10.1016/j.precamres.2019.105582
Reference: PRECAM 105582

To appear in: *Precambrian Research*

Received Date: 19 February 2019
Revised Date: 10 December 2019
Accepted Date: 14 December 2019

Please cite this article as: G. Raymond-Stéphane Koffi, A. Nicaise Kouamelan, M. Ephrem Allialy, Y. Coulibaly, J-J. Peucat, Re-evaluation of Leonian and Liberian events in the geodynamical evolution of the Man-Leo Shield (West African Craton), *Precambrian Research* (2019), doi: https://doi.org/10.1016/j.precamres.2019.105582

Re-evaluation of Leonian and Liberian events in the geodynamical evolution of the Man-Leo Shield (West African Craton)

Gnagnon Raymond-Stéphane KOFFI[a]*, Alain Nicaise KOUAMELAN[a], Marc Ephrem ALLIALY[a], Yacouba COULIBALY[a], Jean-Jacques PEUCAT[b]

[a]UFR-STRM Université F.H.B. Cocody-Abidjan, 22 B.P. 582 Abidjan 22, Côte d'Ivoire

[b] Géosciences Rennes, UMR CNRS 6118, Université de Rennes I, 35042 Rennes CEDEX, France

*Corresponding author at: UFR-STRM Université F.H.B. Abidjan-Cocody, 22 B.P. 582 Abidjan 22, Côte d'Ivoire, E-mail address: koffignagnon@gmail.com ; phone: +22558043409

Abstract

The Leonian (3400–3100 Ma) and Liberian (2850–2700 Ma) events are important magmatic and tectono-metamorphic events in the Archean domain of the Man-Leo Shield in the southern West Africa Craton. The older Leonian event was associated with crust formation, which was variably reworked during the younger Liberian event. In the Man domain of western Côte d'Ivoire, zircon in-situ dating by LA-ICPMS of Granulitic Grey Gneisses (GGGs), the Mangouin charnockite and the Lagoulalé augen orthogneiss allows for the re-evaluation of magmatic and metamorphic activity related to the Leonian and Liberian events. We report here our findings that the GGGs represent the oldest rocks in the study area and formed during the Leonian event. The ages recorded in the GGGs in the Man area are 3156±24, 3098±19, 3093±49 and 3019±53 Ma. The ages of 3156±24 and 3098±19 Ma represent Leonian juvenile magmatism while those of 3093±49 and 3019±53 Ma represent Leonian metamorphism. The ages of the Mangouin charnockite and the Lagoulalé augen orthogneiss are 2798±8 Ma and 2795±9 Ma, respectively, and are interpreted to record peak metamorphic conditions during the Liberian event. Zircon from the augen orthogneiss includes an inherited core with an age of 3121±37 Ma, which corresponds to Leonian GGG ages. This inheritance indicates that the Mangouin charnockite and the Lagoulalé augen orthogneiss were derived either partially or completely from Leonian formations. A previously constrained Sm–Nd model age of 3250 Ma for the charnockite and augen orthogneiss agrees with such a process. The majority of Th/U is higher, indicating a magmatic origin for most zircons. The Leonian and Liberian events are proposed as two distinct events in Man-Leo Shield.

Keywords: Leonian; Liberian; Birimian; tectono-metamorphic event; reworking.

1. Introduction

The Archean Eon represents nearly half of Earth's history, and lasted between 4.0 to 2.5 Ga. It has previously been proposed that more than 50 to 75% of the continental crust differentiated from the mantle during this period (Nelson and Depaolo, 1985; Taylor and McLennan, 1985, Rudnick, 1995: Belousova et al. 2010; Dhuime et al., 2012). However, recent studies support a smaller amount of crustal production, particularly during the Hadean (Fisher and Vervoort, 2018). It is further established that geothermal gradients were also higher in the Archean (Mareschal and Jaupart, 2006). This makes the Archean a particularly interesting period of Earth's history, in terms of petrology and tectonics as well as mineralization. At the petrological level, grey gneisses are a typical Archean lithology, of which TTG orthogneiss suites are a common component that has been the focus of extensive research (Black et al., 1971; Goldich et al., 1970; Hanson et al., 1971; Heimlich and Banks, 1968; Kouvo and Tilton, 1966; Moorbath, 1975; Moorbath et al., 1972, Savanier et al., 2003: Martin et al., 2014).

In the southern West African Craton (WAC), TTGs have been dated to between 3.6 and 3.0 Ga (e.g. Camil, 1984; Potrel et al., 1996; Kouamelan et al., 1997a, 1997b; Thiéblemont et al., 2001; Kouamelan et al., 2015; De Waele et al., 2015; Rollinson, 2016) and inherited zircons are known from 3.7 Ga (Barth et al., 2002; Gouedji et al., 2014; Eglinger et al., 2017). In Côte d'Ivoire, grey gneisses have been dated between 3.2 and 3.0 Ga, and their trace element composition shows TTG characteristics (Kouamelan, 1996; Kouamelan, 1997a, Kouamelan et al., 2015).

In the Archean of the southern West African Craton, two events are recognized based on the "classic" subdivision of e.g. Cahen et al. (1984). The first is the Leonian

(~3.0 Ga) and the second is the Liberian (~2.8 Ga). Furthermore, Camil (1984), Kouamelan (1996) and Kouamelan et al. (1997a) highlighted petrological and geochronological differences between these events in the Man domain. The Leonian (is characterized by banded granulite facies grey gneisses with some metre-thick sheets of Opx-bearing pink granitic granulite (Camil, 1984). The Liberian is characterized by supracrustal rocks in granulite facies. However, De Waele et al. (2015) recently proposed a revision of these two terms based on published age data, where the Leonian refer to early crustal nucleation between ca. 3.5–3.4 Ga, and the Liberian to continuous activity between 3.05–2.65 Ga.

This study presents new geochronological data on granulitic grey gneisses (GGGs), charnockites, and granodiorites from the Man region in western Côte d'Ivoire obtained by in-situ analysis of zircon using Laser-Ablation Inductively-Coupled-Plasma Mass-Spectrometry (LA-ICP-MS). The new data is an improvement upon previous ages obtained from the Man region. These were based on direct evaporation methodologies (Kouamelan et al., 1997a), which can give erroneous results due to partial lead loss or inherited cores, particularly in complex zircon grains. Considering the results obtained in this study, the events in the Man domain are distinguish and a geodynamic model for the evolution of the West African Craton from the Archean to the Paleoproterozoic (Birimian) is discussed.

2. Geological setting

The West African Craton consists of Precambrian formations bordered by mobile belts and sedimentary basins (Fig. 1, Bessoles, 1977; Abouchami et al., 1990; Kouamelan et al., 1997; Egal et al., 2002; Persits et al., 2002; Peucat et al., 2005; Ennih and Liégeois, 2008; Pitra et al., 2010; Baratoux et al., 2011; Schofield et al., 2012; Berger et al., 2013). The basement of the West African Craton is exposed in two shields: the Reguibat Shield in the north and the Man-Leo Shield in the south. Both shields are made up of an Archean and a Paleoproterozoic domain. Previous geochronological studies have identified two major magmatic and tectono-metamorphic events in Archean rocks of the Man-Leo Shield (MacFarlane et al., 1980; Beckinsale et al., 1980; Rollinson and Cliff, 1982; Egal et al., 2002; Bessoles 1977; Cahen et al., 1984; Rollinson 2016). The first event is the Leonian, which was defined in Sierra Leone by McFarlane et al. (1980). Radiometric ages (Pb–Pb, U–Pb and Rb–Sr) place this event between ca. 3.3 Ga and 3.0 Ga (Eberhardt et al., 1962; Beckinsale et al., 1980; Camil, 1984; Thiéblemont et al., 2004). The second event is the Liberian (ca. 2.9–2.7 Ga), which is the most significant metamorphic and magmatic event in the Archean domain of the Man-Leo Shield. The Paleoproterozoic domain (2.27–1.98 Ga) consists of crust formed during the Eburnean megacycle (Tagini, 1971; Bonhomme, 1962; Yacé, 1984; Tempier, 1986; Lemoine, 1988; Sylvester and Attoh, 1992; Feybesse and Milési, 1994; Vidal and Alric, 1994; Ama-Salah et al., 1996; Hirdes and Davis, 2002; Pouclet et al., 2006; Feybesse et al., 2006; Baratoux et al., 2011; De Kock et al., 2012; Parra-Avilla et al., 2016; Grenholm et al., 2019).

The Archean domain of Côte d'Ivoire is located to the west of the Sassandra Fault, which separates it from Paleoproterozoic crust to the east (Fig. 2). Leonian units in Côte d'Ivoire are characterized by grey orthogneiss, pink granulite, anatectic metapelite, and ferriferous quartzites (Camil, 1984). The Leonian formations were reworked during Liberian tectono-metamorphic activity (Kouamelan et al., 1997a), which was associated with high-grade metamorphism, deformation, magmatism, and deposition of supracrustal formations (Beckinsale et al., 1980; MacFarlane et al., 1980; Rollinson and Cliff, 1982; Egal et al., 2002; Rollinson 2016).

Our study area is located in the Man domain, to the west of the Sassandra Fault (Fig. 2). The Man domain, in the narrowest sense, could be limited to the area between parallels 6°N and 8°N and is divided into two domains by the Man-Danané fault. The northern domain is mainly composed of tonalitic grey gneiss, while the southern domain can be subdivided into three sub-domains (Kouamelan et al., 1997a; Kouamelan et al., 2018). These are composed of:

- An intermediate unit (the Danané-Kouibli domain) mainly containing orthopyroxene-bearing migmatitic gneiss.
- The Logoualé band of biotite-bearing migmatitic gneiss and charnockitic gneiss.
- The Toulepleu-Ity unit consisting of metasediments, metavolcanites and granitoids.

3. Methods

We have applied a classic mineral separation procedure to concentrate minerals suitable for U–Th–Pb dating using the facilities available at Geosciences Rennes. Rocks were crushed and only the powder fraction with a diameter of <250 μm was kept. Heavy minerals were concentrated in succession by Wilfley table and heavy liquids. Magnetic minerals were then removed with an isodynamic Frantz separator. Zircon grains were carefully handpicked under a binocular microscope and embedded in epoxy mounts. The grains were then hand-grounded and polished on a lap wheel with a 6 μm and 1 μm diamond suspension successively. The sorted zircon grains are mounted on resin studs. Furthermore, subsequent grinding and polishing exposed the cores of all grains. Optical images of zircons show that they are homogeneous and often oscillatory. Essentially the cores of the zircon grains have been analyzed to have the oldest ages. U–Th–Pb geochronology of zircon was conducted with in-situ Laser-Ablation Inductively-Coupled-Plasma Mass-Spectrometry (LA-ICPMS) at Geosciences Rennes using a ESI NWR193UC excimer laser coupled to a quadrupole Agilent 7700x ICP-MS equipped with a dual pumping system to enhance sensitivity. The instrumental conditions are reported in Table 1. Concordia diagrams and weighted mean calculations were made using Isoplot 4.0 with 2 σ-error and 95% confidence levels (Ludwig, 2008).

4. Sample descriptions

4.1. Granulitic grey gneisses

The granulite grey gneiss samples (GGGs) studied here are labeled YAL-1 and TON-1. Petrographic descriptions of these rocks are summarized in Table 2 and presented in detail in Kouamelan 1996; Kouamelan et al., 1997. Two main morphologies can be distinguished among the zircons of the GGGs. There are (i) elongated grains with generally blunt tips and (ii) round grains with multiple facets. Elongated zircons have a magmatic zoning and sometimes a core. They have a very irregular surface. Shallow cavities can be observed along the grain margins. The absence of faces could be the result of the extreme conditions imposed during granulite metamorphism. Round zircons generally do not have a core though magmatic zoning can still be observed (Kouamelan, 1996).

4.2. Augen orthogneiss and the charnockite

The main features of these rocks are summarized in Table 2. Zircons of the augen orthogneiss and the charnockite have comparable morphologies. They are elongated and euhedral with rounded tips and generally > 150 µm. They correspond to the high-temperature S24/25 zircon types according to the Pupin (1980) classification; no cores have been observed.

5. Results

5.1. YAL-1: grey granulitic orthogneiss

Twenty-two zircons spots were analyzed and can be divided into three groups based on $^{207}Pb/^{206}Pb$ (Table 3). In group 1, seven concordant spots yield an average $^{207}Pb/^{206}Pb$ ages of 3098±19 Ma (MSWD=0.27; n=7). In group 2, one concordant spot gives a $^{207}Pb/^{206}Pb$ date of 3019±53 Ma (Fig. 3). The first age is interpreted to correspond to magmatic crystallization while the second would represent partial Pb-loss or metamorphism during the Leonian event. In group 3, six zircon spots yield younger $^{207}Pb/^{206}Pb$ ages of ca. 2814–2791 Ma and define an upper intercept age of 2812±14 Ma (MSWD=0.91; n=6, Fig. 3). This age is interpreted to represent metamorphic overprinting at ca. 2.8 Ga associated with the Liberian event. The zircon spots of this group also define a lower intercept age of 189±308 Ma (Fig. 3). We attribute this lower intercept to thermal disturbance linked to mafic CAMP magmatism (e.g. Deckart et al., 2005; Whalen et al., 2015). These zircons show considerable variation in both Th and U concentrations and yield Th/U of 0.14-0.98.

5.2. TON-1: grey granulitic orthogneiss

Sixteen zircon grains were analyzed and three U–Pb age groups are defined based on $^{207}Pb/^{206}Pb$ (Table 3). In group 1, four concordant spots give an average of $^{207}Pb/^{206}Pb$ ages of 3156±24 Ma (MSWD= 0.73; n=4). In group 2, one concordant spot gives a $^{207}Pb/^{206}Pb$ ages of 3093±49 Ma (Fig. 4). Like in sample YAL-1, the first age is interpreted to correspond to the magmatic crystallization of this rock and the second represent an event of partial Pb-loss or metamorphism during the Leonian. In group 3, two zircon grains yield younger concordant $^{207}Pb/^{206}Pb$ ages between 2825–2805 Ma, which define an average $^{207}Pb/^{206}Pb$ ages of 2806±25 Ma (MSWD=0.25; n=2, Fig. 4). The age defined by group 3 zircon grains is interpreted to record metamorphic overprinting during the Liberian event. The analyzed zircons mostly preserve magmatic oscillatory zoning and commonly exhibit high Th/U from 0.14 to 0.98, excluding spots 9, 16 and 25 (0.05, 0.09 and 0.09 respectively).

5.3. MANG-1: charnockite

Twenty-six spots on twenty-four zircon grains from charnockite rock sample MANG-1 (Table 3) were analyzed. The twenty-six concordant spots (>95%) define an average $^{207}Pb/^{206}Pb$ ages of 2798±8 Ma (MSWD=0.59; n=26, Fig. 5). It is interpreted to represent the crystallization age of the charnockite. The analyzed zircon domains are characterized by high Th/U (0.32-1.07).

5.4 LAG-1: augen orthogneiss

Twenty-two spots on twenty zircon grains of the augen orthogneiss sample LAG-1 (Table 3) were analyzed. All concordant spots (>95%) with near-absent lead-loss define an average $^{207}Pb/^{206}Pb$ ages of 2795±9 Ma (MSWD=1.01; n=22, Fig. 6). This age is taken to represent the crystallization age of this rock. One zircon (spot 18) yields an older $^{207}Pb/^{206}Pb$ date of ca. 3121 Ma, suggesting inheritance. All analyzed zircon domains have Th/U >0.1, which are typical for magmatic zircon (Williams and Claesson, 1987), excluding spot 34 (0.08).

6. Discussion

6.1. The Leonian event: juvenile magmatism

The ages obtained in this study (Table 3) are consistent with those reported by Camil (1984) and Kouamelan et al. (1997a) from the same area, using the TIMS method on zircon populations and single-zircon evaporation, respectively. The ages of 3156±24, 3098±19, 3093±49, and 3019±53 Ma for the granulitic grey gneisses (GGGs) are Leonian and represent the oldest ages in our study area. These data indicate a period of magmatic activity between ca. 3160–3100 Ma, followed by Leonian metamorphism between ca. 3100–3000 Ma. The ages recorded by the GGGs at 2812±14 and 2806±25 Ma record the effect of Liberian metamorphism. In the Man domain, these rocks have whole-rock Nd model ages between 3.3 and 3.2 Ga (Kouamelan et al., 1997a). We suggest that the Leonian event was dominated by juvenile magmatism with limited crustal recycling. Rollinson (2016) in his synthesis of Archean geology in Sierra Leone, Liberia, Guinea, and Côte d'Ivoire highlights rocks formed at 3.26–3.05 Ga. Leonian event is thereby present throughout the WAC.

6.2. The Liberian event: reworking of Leonian crustal components

The Manguoin charnockite dated at ca. 2798 Ma and the Lagoulalé augen orthogneiss of ca. 2794 Ma have coeval ages and may have formed during peak metamorphism during the Liberian event. The end of this tectono-metamorphic event occurred around 2740 Ma, which corresponds to the whole rock-garnet Sm–Nd age of a granulitic pink granite sampled in same area (Kouamelan et al., 1997a). The Manguoin charnockite and the Lagoulalé augen orthogneiss have previously constrained whole-rock Nd model ages of about 3250 Ma (Kouamelan, 1996), which predates their emplacement ages by ca. 450 Ma. This implies that the Manguoin charnockite and Lagoulalé augen orthogneiss were sourced from older Mesoarchean crust. This is also supported by the inherited zircon in the augen orthogneiss of LAG-1, which records a $^{207}Pb/^{206}Pb$ age of 3121±37 Ma. This inherited age is a minimum and approximately 100 Ma younger than the Nd model age. Moreover, this inherited age corresponds to the age of the GGGs. In view of the above, it can be ascertained that the Liberian formations have Leonian protoliths. The latter are most certainly juvenile lithological assemblages given the small age difference with the Nd model age. In the Reguibat Shield, Potrel et al. (1998) reported ages of charnockitic granite ranging between 2.9–2.7 Ga with Nd model ages between 3.2–3.1 Ga. These rocks have positive εNd (3.0), in agreement with a juvenile origin for Leonian rocks. Thus, the Liberian event succeeded the Leonian event, and was associated with significant crustal reworking. The presence of granulite sheets within the GGGs, particularly in the TON-1 rock, shows that they were subjected to high-grade metamorphism (Kouamelan et al., 1997a; Kouamelan, 1996).

The data indicate that distinct magmatic events occurred during Leonian (3.3–3.0 Ga) and Liberian (2.8–2.7 Ga) times. These same events are recognized across the Archean domain in the Man-Leo Shield, including in eastern Guinea (Bering et al., 1998; Thiéblemont et al., 2004), Liberia (Hurley et al., 1971), and Sierra Leone (Barth et al., 2002). They are also recorded in the Reguibat Shield in the northern West African Craton (Fig. 1, Potrel et al., 1996, 1998; Schofield et al., 2012; Montero et al., 2014). This indicates that the Leonian and Liberian were regionally significant events.

Our data contradict De Waele et al. (2015) who proposed a revision of the terms Leonian and Liberian, with the Leonian referring to Paleoarchean crustal nucleation between 3.55–3.40 Ga, while the Liberian represent continuous crustal growth between ca. 3.05–2.6 Ga. The presence of inherited zircons in the younger suite and their Nd model age ranging to 3.4–3.3 Ga indicate reworking of the older gneisses (Rollinson, 2016). At present time, there is no knwon juvenile magmatism at 2.7–2.8

Ga. Although Paleoarchean ages have not been found yet in the Man Shield of Côte d'Ivoire, we argue that the Leonian and Liberian are two distinctive events.

6.3. Leonian and Liberian events in the geodynamical evolution of the Man Shield

The oldest ages recorded in the WAC range from 3.7–3.5 Ga and are scarce. These are mostly inherited ages (Barth et al., 2002; Gouédji et al., 2014; Eglinger et al., 2017; Asiedu et al., 2017; Parra-Avilla et al., 2017; Petersson et al., 2016; 2017, 2018), except for the scarce crustal segments present in the Mauritanian part of the Reguibat Shield (Potrel et al., 1996) and in the Guinean part of the Man-Leo Shield (Thiéblemont et al., 2001). In Sierra Leone, Barth et al. (2002) reported an age of 3.44 Ga (Re–Os on whole rock) on rocks that the authors described as eclogite. The formations frequently encountered in the Man domain and elsewhere in the Archean of the WAC are the granulitic grey gneisses (GGGs) and paragneisses like kinzigite. The latter are often associated with magnetite bearing quartzites and amphibole-pyroxenites. GGGs are therefore the oldest rocks in the WAC after the rare relics highlighted by Potrel et al. (1996) and Thiéblemont et al. (2001). Based on the results obtained in this work and considering the Nd model ages of the GGGs (Kouamelan et al., 1997a), the Leonian event can be considered as occurring in the range of ca. 3.4 to 3.1 Ga. Most of the ages obtained on the gneissic formations in the Man-Leo and Reguibat Shields actually belong to this range (Kouamelan et al., 1997a; Potrel et al., 1998; Barth et al., 2002; Thiéblemont et al., 2004). However, we would assign the older ages (3.7-3.4 Ga) to pre-Leonian phase. This age range of 300 Ma could demonstrate the existence of many small continental crustal blocks that evolved separately during this period. We consider the younger ages in the Leonian rocks between 3.1 and 3.0 Ga to be mainly due to metamorphism, because they are few and in the samples YAL-1 and TON-1 of this study overprint the older ages. The characteristics of these metamorphic and/or tectonic episodes need to be demonstrated in subsequent work, and to what extent they were responsible for the deformation of Leonian formations.

After the Leonian, the Liberian event is the major tectono-metamorphic and magmatic event in the Archean domain of the WAC. As opposed to Leonian formations which are systematically gneissic, the Liberian formations can be undeformed such as the Mangouin charnockite or the Yorogué granodiorite, or weakly deformed such as the Lagoualé augen orthogneiss (Table 2; Camil, 1984; Kouamelan, 1996). The ages of the Liberian formations in Côte d'Ivoire are grouped in a smaller range (2.8–2.7 Ga), compared to that of the Leonian formations. An important characteristic of the Liberian formations is that they are sourced from Leonian crust. This is supported by their negative ε_{Nd} at 2.8 Ga and Nd model ages ranging between 3.3 and 3.1 Ga (Kouamelan et al., 1997a; Potrel et al., 1998). The presence of inherited zircon with Leonian ages highlighted in this study corroborates the crustal signature of the Liberian rocks. The second characteristic is that the dating of the different facies of the Liberian rocks allows to constrain the high-grade and retrograde phase of this metamorphic event. Thus, the Mangouin charnockite dated at 2798±8 Ma characterizes the paroxysm of Liberian metamorphism (Kouamelan et al. 1997a), while Touijenjert granites (2726±7 Ma) in the Reguibat Shield (Potrel et al., 1998) characterizes the retrograde phase. However, the temporal difference between the Mangouin and Touijenjert intrusions may also be a reflection of diachronous processes, where metamorphism and magmatism occurred at different times across the Archean crust.

In terms of geodynamics, we propose that the Liberian event represents a collisional phase between Leonian crustal blocks. The Liberian magmatism that followed was highly contaminated by the Leonian crust. This model makes it possible to clearly distinguish between the Leonian and Liberian events that we highlight in the Man domain. The Archean continent was subsequently affected by the tectonic and magmatic events that were associated with the Birimian crust (Kouamelan et al., 1997a, Thiéblemont et al., 2004). The age of 180±380 Ma defined by the lower intercept of sample YAL-1 is close to the age of the ca. 200 Ma CAMP magmatism associated with the opening of the Atlantic Ocean, which also affected the crust in the Kenema-Man craton (e.g. Deckart et al., 2005; Whalen et al., 2015).

7. Conclusions

LA-ICP-MS in-situ U–Pb dating has been performed on zircons from the granulitic grey gneiss (3.15–3.01 Ga), the Mangouin charnockite and the Lagoulalé augen orthogneiss (2.8 Ga) located in the Archean domain of western Côte d'Ivoire. This has allowed for the reassessment of the Leonian and Liberian events in the geodynamic evolution of the West African Craton. GGGs crystallized during the Leonian event, which corresponds to juvenile magmatism with subsequent metamorphism over a period of 300 million years (3.4–3.1 Ga). The GGGs represent the oldest rocks in the Man domain. The Mangouin charnockite and the Lagoulalé augen orthogneiss formed during the Liberian tectono-metamorphic and magmatic event (2.85–2.7 Ga). Liberian magmatism corresponds to the reworking of Leonian juvenile units. These Leonian juvenile units collided during the Liberian event. Liberian magmatism was strongly contaminated by the Leonian crust. The Leonian and Liberian events are distinct events in the Man-Leo Shield.

Acknowledgements

The authors are very grateful to C. Delor (BRGM), Y. Simeon (ANTEA-Orleans), Pr J. Camil (SODEMI) and Dr. B.D. Yao (Direction de la Géologie-Abidjan) for their material and financial support through the French FAC II project involving the Direction de la Géologie (Côte d'Ivoire) and the BRGM (France). We are also grateful to J-L. Paquette and M. Poujol for their help in geochronological data acquisition. The manuscript was substantially improved by constructive comments from three reviewers: G.S. de Kock, M. Grenholm and A. Petersson and proofreading of Ph. Rodenbough. Finally, the editorial handling of the journal editors, Prof. W. Teixeira is deeply appreciated.

References

Abouchami, W., Boher, M., Michard A., Albarede, F., 1990. A major 2.1 Ga old event of mafic magmatism in West Africa: An early stage of crustal accretion. Journal Geophysical Research Letter 95, 17605-17629.

Ama-Salah, I., Liegeois, J.P. and Pouclet, A., 1996. Evolution d'un arc insulaire océanique birimien précoce au Liptako nigérien (Sirba): géologie, géochronologie et géochimie. Journal of African Earth Sciences 22, 235-254.

Asiedu, D.K., Asong, S, Atta-Peters D., Sakyi P.A., Dampare S.B., Anani C.Y., Ben-Xun S., 2017. Geochemical and Nd-isotopic compositions of juvenile-type Paleoproterozoic Birimian sedimentary rocks from southeastern West African Craton (Ghana): Constraints on provenance and tectonic setting. Precambrian Research 300, 40–52.

Baratoux, L., Metelka, V., Naba, S., Jessell, M.W., Grégoire, M., Ganne, J., 2011. Juvenile Paleoproterozoic crust evolution during the Eburnean orogeny (2.2–2.0 Ga), western Burkina Faso. Precambrian Research 191, 18–45.

Barth, M.G., Rudnick, R.L., Carlson R.W. Horn I. McDonough W. F., 2002. Re-Os and U-Pb geochronological constraints on the eclogite-tonalite connection in the Archaean Man Shield, West Africa. Precambrian Research 118, 267–283.

Beckinsale, R.D., Gale, N.H., Pankhurst, R.J., Macfarlane, A., Crow, M.J., Arthurs, J.W., Wilkinson, A.F., 1980. Discordant Rb–Sr and Pb–Pb whole rock isochron for the Archaean basement of Sierra Leone. Precambrian Research 13, 63–76.

Belousova, E. A., Kostitsyn, Y. A., Griffin, W. L., Begg, G. C., O'Reilly, S. Y., Pearson, N. J. 2010., The growth of the continental crust: Constraints from zircon Hf-isotope data. Lithos, 119, 457–466. doi:10.1016/j.lithos.2010.07.024.

Berger, J., Diot, H., Lo, K., Ohnenstetter, D., Féménias, O., Pivin, M., Charlier, B., 2013. Petrogenesis of Archean PGM-bearing chromitites and associated ultramafic–mafic–anorthositic rocks from the Guelb el Azib layered complex (West African craton, Mauritania). Precambrian Research 224, 612–628.

Bering, D., Brinckmann, J., Camara, N., Diawara, M., Gast, L., Kieta, S., 1998. Evaluation de l'Inventaire des Resources Minerals de Guinee. In: Cooperation Technique Republique de Guinea-Republique Federal d'Allemagne, Project 94.2025.8. BGR, Hannover, p. 109.

Bessoles, B., 1977. Géologie de l'Afrique. Le craton Ouest-africain. Mémoire BRGM. no 88. 402p.

Black, L.P., Gale, N.H., Moorbath, S., Pankhurst, R.J., McGregor, V.R., 1971. Isotopic dating of very early Precambrian amphibolite facies gneisses from the

Godthaab district, West Greenland. Earth and Planetary Science Letters 12. 245-259.

Bonhomme M., 1962. Contribution à l'étude géochronologique de la plate- forme de l'Ouest africain. Annales de la Faculté des Sciences, Université de Clermont-Ferrand 5, 62p.

Cahen, L., Snelling, N.J., Delhal, J., Vail, J.R., 1984. The Geochronology and Evolution of Africa. Clarendon Press, Oxford.

Camil, J., 1984. Pétrographie, chronologie des ensembles granulitiques archéens et formations associées de la région de Man (Côte d'Ivoire). Implications pour l'histoire géologique du craton Ouest Africain. Thèse Doctorat Ès Sciences. Université Abidjan, 306p.

Deckart, K., H. Bertrand, and J.-P. Liegeois, 2005. Geochemistry and Sr, Nd, Pb isotopic composition of the Central Atlantic Magmatic Province (CAMP) in Guyana and Guinea, Lithos, 82(3), 289–314.

De Kock, G.S., Théveniaut, H., Botha, P.M.W., Gyapong, W., 2012. Timing the structural events in the Paleoproterozoic Bolé-Nangodi belt terrane and adjacent Maluwe basin, West African Craton, in central-west Ghana. Journal of Africa Earth Sciences. 65, 1–24.

De Waele, B., Lacorde, M., Vergara, F., Chan, G., 2015. New insights on Proterozoic tectonics and sedimentation along the peri-Gondwanan West African margin based upon U–Pb SHRIMP geochronology. Precambrian Research 259, 156–175.

Dhuime, B., Hawkesworth, C. J., Cawood, P. A., & Storey, C. D., 2012. A Change in the Geodynamics of Continental Growth 3 Billion Years Ago. Science 335 (6074), 1334–1336. doi:10.1126/science.1216066.

Eberhardt, P., Geiss, J., Houtermans, F.G., Signer, P., 1962. Age determination on lead ores. Geologische Rundschau 52, 836–852.

Egal, E., Thiéblemont, D., Lahondére, D., Guerrot, C., Costea, C.A., Iliescu, D., Delor, D., Goujou, J.-C., Lafon, J.M., Tegyey, M., Diaby, S., Kolié, P., 2002. Late Eburnean granitization and tectonics along the western and northwestern margin of the Archean Kénéma-Man domain (Guinea, West African Craton). Precambrian Research.117, 57–84.

Eglinger, A., Thébaud, N., Zeh, A., Davis, J., Miller, J., Parra-Avila, L.A., Loucks, R.,McCuaig, C., Belousova, E., 2017. New insights into the crustal growth of the Paleoproterozoic margin of the Archean Kéména-Man domain, West African craton (Guinea): Implications for gold mineral system. Precambrian Res. 292, 58–289.

Ennih, N., Liégeois, J.P., 2008. The boundaries of the West African Craton, with special reference to the basement of the Moroccan metaCratonic Anti-Atlas belt. In: Ennih, N., Liégeois, J.P. (Eds.). The Boundaries of the West African Craton. The Geological Societyof London Special Publication 297, 1–17.

Feybesse, J.L., Milési, J.-P., 1994. The Archean/Paleoproterozoic contact zone in West Africa: a mountain belt of décollement thrusting and folding on a continental margin related to 2.1 Ga convergence of Archean Cratons? Precambrian Research 69,199–227.

Feybesse, J.L., Billa, M., Guerrot, C., Duguey, E., Lescuyer, J.L., Milési, J.P., Bouchot, V., 2006. The Paleoproterozoic Ghanaian province: geodynamic model and ore controls, including regional stress modeling. Precambrian Research 149,149–196.

Fisher, C. M., Vervoort, J. D., 2018. Using the magmatic record to constrain the growth of continental crust—The Eoarchean zircon Hf record of Greenland. Earth and Planetary Science Letters, 488, 79–91. doi:10.1016/j.epsl.2018.01.031.

Goldich, S.S., Hedge, C.E., Stern, T.W., 1970. Age of the Morton and Montevideo gneisses and related rocks, southwestern Minnesota. Geological Society of America Bulletin 81, 3671–3996.

Gouedji, F., Picard, C., Coulibaly, Y., Audet, M.-A., Auge, T., Goncalves, P., Paquette, J.L.,Ouattara, N., 2014. The samapleu maficeultramafic intrusion and its NiCuPGE mineralization: an Eburnean (2.09 Ga) feeder dyke to the Yacouba layered complex (Man Archean craton, western Ivory Coast). Bull. Soc. Geol. Fr. 185, 393-411.

Gorman, B.E., Pearce, T.H., Birkett, T.C., 1978. On the structure of Archaean greenstone belts. Precambrian Research 6, 23–41.

Grenholm, M., Jessell, M., Thébaud, N., 2019. A geodynamic model for the Paleoproterozoic (ca. 2.27–1.96 Ga) Birimian Orogen of the southern West African Craton – Insights into an evolving accretionary-collisional orogenic system. Earth-Science Reviews. doi:10.1016/j.earscirev.2019.02.006.

Hanson, G.N., Goldich, S.S., Arth, J.G., Yardley, D.H., 1971. Age of the early Precambrian rocks of the Saganaga Lake–Nothern Light Lake area, Ontario–Minnesota. Canadian Journal of Earth Sciences 8, 1110–1124.

Heimlich, R.A., Banks, P.O., 1968. Radiometric age determinations, Bighorn Mountains, Wyoming. American Journal of Science 266, 180–192.

Hirdes, W., Davis, D.W., 2002. U–Pb geochronology of Paleoproterozoic rocks in the southern part of the Kedougou-Kéniéba Inlier, Senegal. West Africa: evidence for diachronous accretionary development of the Eburnean Province. Precambrian Research 118, 83–99.

Hurley, P.M., Leo, G.W., White R.W., Fairbairn H.W., 1971. Liberian Age Province (about 2,700 m.y.) and Adjacent Provinces in Liberia and Sierra Leone. GSA Bulletin 82, 3483-3490.

Jahn, B.M., Glikson, A.Y., Peucat, J.J., Hickman, A.H., 1981. REE geochemistry and isotopic data of Archaean silicic volcanics and granitoids from the Pilbara Block, western Australia: implications for the early crustal evolution. Geochimca et Cosmochimca Acta 45, 1633-1652.

Kouamelan, A.N., 1996. Géochronologie et géochimie des formations archéennes et protérozoïques de la dorsale de Man en Côte d'Ivoire, implication pour la transition archéen-protérozoïque. Thèse de Doctorat Université de Rennes, France, 227p.

Kouamelan, A.N., Delor, C., Peucat, J.-J., 1997a. Geochronological evidence for reworking of Archaean terrains during the Early Proterozoic (2.1 Ga) in the western Côte d'Ivoire (Man Shield – West African Craton). Precambrian Research 86, 177–199.

Kouamelan, A.N., Peucat, J.-J., Delor, C., 1997b. Reliques archéennes (3.15 Ga) au sein du magmatisme birimien (2.1 Ga) de Côte d'Ivoire, craton ouest-africain. Compte Rendu de l'Académie Sciences Paris 324, 719–727.

Kouamelan, A.N., Djro S.C., Allialy, M.E., Piquette J-L., Peucat J-J., 2015. The oldest rock of Ivory Coast, Journal of African Earth Sciences 103, 65–70.

Kouamelan, A. N., Kra, K. S. A., Djro, S. C., Paquette, J.-L.,Peucat, J.-J., 2018. The Logoualé Band: A large Archean crustal block in the Kenema-Man domain (Man-Leo rise, West African Craton) remobilized during Eburnean orogeny

(2.05 Ga), Journal of African Earth Sciences, https://doi.org/10.1016/j.jafrearsci.2017.09.004.

Kouvo, O., Tilton, G.R., 1966. Mineral ages from the Finnish Precambrian. Journal of Geology 74, 421–442.

Lemoine S., 1988. Evolution géologique de la région de Dabakala (NE de la Côte d'Ivoire) au protérozoïque. Possibilités d'extension au reste de la Côte d'Ivoire et au Burkina Faso : similitudes et différences; les linéaments de Greenville-Ferkéssedougou et Grand Cess-Niakaramandougou. Thèse d'Etat, Université Clermont-Ferrand, 334p.

Ludwig K., 2008. Isoplot 4.00 beta, rev. 10 Sept, 2008. Berkeley Geochronology Centre.

MacFarlane, A., Crow, M.J., Arthurs, J.W., Wilkinson, A.F., 1980. The geology and mineral resources of northern Sierra Leone. Institute of Geological Sciences Overseas Membership. 7, 134p.

Mareschal, J.C., Jaupart, C., 2006. Archean thermal regime and stabilization of cratons. In. Benn, K., Mareschal, J.-C., Condie, K, editors, Archean geodynamics and environments, volume 164 of monographs, pages 61–73. AGU.

Martin, H., Moyen, J.-F., Guitreau, M., Blichert-Toft, J., Le Pennec, J.-L. 2014. Why Archaean TTG cannot be generated by MORB melting in subduction zones. Lithos, 198-199, 1–13. doi:10.1016/j.lithos.2014.02.017.

Montero, P., Haissen, F., El Archi, A., Rijmati, E., Bea, F., 2014. Timing of Archaean crust formation and cratonisation in the Awsard-Tichla zone of the NW Reguibat Shield, West African Craton: a SHRIMP, Nd–Sr isotopes and geochemical reconnaissance study. Precambrian Research. 242, 112–137.

Moorbath, S., 1975. Evolution of Precambrian crust from strontium isotopic evidence. Nature 254, 395–398.

Moorbath, S., O'Nions, R.K., Pankhurst, R.J., Gale, N.H., McGregor, V.R., 1972. Further rubidium–strontium age determinations on the very eary Precambrian rocks of Godthaab region, West Greenland. Nature 240, 78–82.

Nelson, B. K., Depaolo, D.J., 1985. Rapid production of continental crust1.7 to 1.9 by ago: Nd isotopic evidence from the basement of North America Midcontinent. Geological Society of America Bulletin 96, 746-754.

Nisbet, E G., Cheadie, M.J., Arndt, N.T., Bickle, M. J., 1993. Constraining the temperature of the Archean mantle: a review of evidence from komatiites. Lithos 30, 291-307.

Parra-Avilla, L.A., Belousova, E., Fioentini, M.L., Baratoux, L., Davies, J., Miller, J., McCuig, T.C., 2016. Crustal evolution of the Palaeoproterozoic Birimian terranes of the Baoule-Mossi domain, southern West African Craton: U–Pb and Hf-isotope studies of detrital zircons. Precambrian Research 274, 25–60.

Parra-Avila, L.A., Kemp, A.I., Fiorentini, M.L., Belousova, E., Baratoux, L., Block, S., Jessell, M., Bruguier, O., Begg, G.C., Miller, J., Davis, J., 2017. The geochronological evolution of the Paleoproterozoic Baoulé-Mossi domain of the Southern West African Craton. Precambrian Research. 300, 127.

Parra-Avila, L. A., Belousova, E., Fiorentini, M. L., Eglinger, A., Block, S., & Miller, J., 2018. Zircon Hf and O-isotope constraints on the evolution of the Paleoproterozoic Baoulé-Mossi domain of the southern West African Craton. Precambrian Research, 306, 174–188. doi:10.1016/j.precamres.2017.12.044.

Persits, F., Ahlbrandt, T., Tuttle, M., Charpentier, R., Brownfield, M., Takahashi, K., 2002. Map showing geology, oil and gas fields and geological provinces of

Africa, ver. 2.0. USGS Open File Report 97-470A, http://pubs.usgs.gov/of/1997/ofr-97470/OF97 470A/index.html (accessed 6.7.13).

Petersson, A., Scherstén, A., Kemp, A.I.S., Kristinsdóttir, B., Kalvig, P., Annum, S., 2016. Zircon U-Pb-Hf evidence for subduction related crustal growth and reworking of Archaean crust within the Palaeoproterozoic Birimian terrane, West African Craton, SE Ghana. Precambrian Research. 275, 286–309. http://dx.doi.org/10.1016/j.precamres. 2016.01.006.

Petersson, A., Scherstén, A., Gerdes, A., 2017. Extensive reworking of Archaean crust within the Birimian terrane in Ghana as revealed by combined zircon U–Pb and Lu–Hf isotopes. Geoscience. Frontiershttp://dx.doi.org/10.1016/j.gsf.2017.02.006.

Petersson, A., Scherstén, A., Kristinsdóttir, B., Kemp, A. and Whitehouse, M., 2018. Birimian crustal growth in the West African Craton: U-Pb, O and Lu-Hf isotope constraints from detrital zircon in major rivers.Chemical Geology, 479, pp.259-https://doi.org/10.1016/j.chemgeo.2018.01.021.

Peucat, J.J., Capdevila, R., Drareni, A., Mahdjoub, Y., Kahoui, M., 2005. The Eglab massif in the West African Craton (Algeria), an original segment of the Eburnean orogenic belt: petrology, geochemistry and geochronology. Precambrian Research 136 (2005) 309–352.

Peucat, J.-J., Jayananda, M., Chardon, D., Capdevila, R., Fanning, C. M., & Paquette, J.-L., 2013. The lower crust of the Dharwar Craton, Southern India: Patchwork of Archean granulitic domains. Precambrian Research, 227, 4–28. doi:10.1016/j.precamres.2012.06.009.

Pitra, P., Kouamelan, A.N., Ballevre, M., Peucat, J.J., 2010. Palaeoproterozoic high-pressure granulite overprint of the Archean continental crust: evidence for homogeneous crustal thickening (Man Shield, Ivory Coast). Journal of metamorphic Geology, 2010, 28, 41–58.

Potrel, A., Peucat, J.J., Fanning, M., Auvray, B., Burg, J.P., Caruba, C., 1996. 3.5 Ga old terranes in the West African Craton, Mauritania. Journal of the Geological Society, London, 153, 507–510.

Potrel, A., Peucat, J. J. and Faning C. M., 1998. Archean crustal evolution of the West African Craton: example of the Amsaga Area (Reguibat Rise). U-Pb and Sm–Nd evidence for crustal growth and recycling. Precambrian Research90, 107-117.

Pouclet, A., Doumbia, S., Vidal, M., 2006. Geodynamic setting of the Birimian volcanism in central Ivory Coast (western Africa) and its place in the Palaeoproterozoic evolution of the Man shield. Bulletin de la Société Geologique de France 177,105–121.

Pupin, J.P., 1980. Zircon and granite petrology. Contributions to Mineralogy and Petrology. 73, 207–220. Rollinson, H., 2016. Archaean crustal evolution in West Africa: A new synthesis of the Archaean geology in Sierra Leone, Liberia, Guinea and Ivory Coast. Precambrian Research. 281, 1–12.

Rollinson, R.H, Cliff, R.A., 1982. New Rb Sr age determin- ations on the Archaean basement of eastern Sierra Leone. Precambrian Research. 17, 63 72.

Rudnick, R. L., 1995. Making continental crust. Nature, 378, p. 571-577.

Savanier, D., Guille, G., Maury, R.C., Blais, S., Guillou, H., Legendre, C., Rossi, P., 2003. Geology, petrology and radiochronology of Nuku Hiva (Marquesas Island, French Polynesia). EGS – AGU – EUG Joint Assembly, Nice, France, 6 – 11, April 2003, Abstract id. 1105.

Schofield, D.J., Horstwood, M.S.A., Pitfield, P.E.J., Gillespie, M., Darbyshire, F., O'Connor, E.A., Abdouloye, T.B., 2012. Precambrian Research. 204–5, 1–11.

Sylvester, P.J., Attoh, K., 1992. Lithostratigraphy and composition of 2.1 Ga greenstone belts of the West African Craton and their bearing on crustal evolution and the Archean-Proterozoic boundary. Journal of Geology. 100,377–392.

Tagini B., 1971. Esquisse structurale de la Côte d'Ivoire. Essai géotectonique régionale. Thèse d'Etat Université de Lausanne. SODEMI, Bulletin. N°5, 302p.

Taylor, S.R., McLennan, S.M., 1985. The continental crust: its composition and evolution. Blackwell scientific Publications, Oxford, 312 p.

Tempier P., 1986. Le Burkinien : cycle orogénique majeur du protérozoïque inférieur en Afrique de l'Ouest. Publication occasionnelle. CIFEG, n°10, pp. 17-23.

Thiéblemont, D., Delor, C., Cocherie, A., Lafo, J.M., Goujou, J.C., Balde, A., Bah, M., Sane, H., Fanning, C.M., 2001. A 3.5 Ga granite-gneiss basement in Guinea: further evidence for early Archaean accretion within the West African Craton. Precambrian Research, 108, 179–194.

Thiéblemont, D., Goujou, J.C., Egal, E., Cocherie, A., Delor, C., Lafon, J.M., Fanning, C.M., 2004. Archaean evolution of the Leo Shield and its Eburnean reworking. Journal of Africa Earth Sciences. 39, 97–104.

Vidal, M., Alric, G., 1994. The Paleoproterozoic (Birimian) of Haute-Comoé in the West African Craton, Ivory Coast: a transtensional back-arc basin. Precambrian Research. 65, 207–229.

Whalen, L., E. Gazel, C. Vidito, J. Puffer, M. Bizimis, W. Henika, and M. J. Caddick, 2015. Supercontinental inheritance and its influence on supercontinental breakup: The Central Atlantic Magmatic Province and the break up of Pangea, Geochem. Geophys. Geosyst., 16, doi:10.1002/2015GC005885.

Whitney, D.L., Evans, B.W., 2010. Abbreviations for names of rock-forming minerals. American Mineralogist 95, 185–203.

Yace I., 1984. Le précambrien de l’Afrique de l’Ouest et ses corrélations avec le Brésil Oriental. Rapport final, Publication PICG-CIFEG, n°2, Paris, 28p.

Laser-ablation system ESI NWR193UC	
Laser type/wavelength	Excimer 193 nm
Pulse duration	<5ns
Energy density on target	~7 J/cm
ThO^+/Th^+	<0.5%
He gas flow	~800 ml/min
N_2 gas flow	4 ml/min
Laser repetition rate	3–5 Hz (zircon)
Laser spot size	26–44 µm (zircon)
ICP-MS Agilent 7700x	
RF power	1350 W
Sampling depth	5.0–5.5 mm (optimized daily)
Carrier gas flow (Ar)	~0.85 l/min (optimized daily)
Coolant gas flow	16 l/min
Data acquisition protocol	Time-resolved analysis
Scanning mode	Peak hopping, one point per peak
Detector mode	Pulse counting, dead time correction applied, and analog mode when signal intensity >~106 cps
Isotopes determined	^{204}(Hg+Pb), ^{206}Pb, ^{207}Pb, ^{208}Pb, ^{232}Th, ^{238}U
Dwell time per isotope	10 ms (30 ms for ^{207}Pb)
Sampler, skimmer cones	Ni
Extraction lenses	X type

Table 1 : Operating conditions for the LA-ICP-MS equipment.

Sample	YAL-1	TON-1	MANG-1	LAG-1
Lat. (N) Long. (W)	7°46'19.8" 7°33'42.6"	7°26'37.2" 7°36'53.9"	7°38'27.6" 7°36'37.8"	7°14'11.7" 7°46'51.3"
Rock type	Granulitic grey gneiss	Granulitic grey gneiss	Charnockite	Augen orthogneiss
Mineral composition (main accessories)	Qz and perthitic Kf + Opx, Cpx, Bt (Zircon and opaques)	Qz and perthitic Kf + Opx, Cpx, biotite (Zircon and opaques)	Kf and Qz + Pl, Opx, Cpx. antiperthitic Pl, mesoperthitic Kf. (Chl, Bt, zircon, monazite, opaques)	Porphyritic Qz and Kf + Ferromagnesian (Hbl, Bt). (Sphene, epidote, zircon and apatite)
Rock type classification (Barker and Arth, 1976)				
An-Ab-Or	Tonalitic	Tonalitic	Tonalitic	Granodioritic
K-Na-Ca	Trondjhemitic trend	Trondjhemitic trend	Trondjhemitic trend	Calc-alkaline trend
Structure	banded	banded	Undeformed	Sheared, foliation N75° dextral shearing N60°

Table 2: Summary of main features of the studied rocks. Abbreviations after Whitney and Evans 2010.

Analysis	Grain Spot	U (ppm)	Th (ppm)	Pb (ppm)	Th/U	Isotopic ratios						Age Ma						Conc (%)
						$^{207}Pb/^{235}U$	± 2σ (abs)	$^{206}Pb/^{238}U$	± 2σ (abs)	$^{207}Pb/^{206}Pb$	± 2σ (abs)	$^{206}Pb/^{238}U$	± 2σ	$^{207}Pb/^{235}U$	± 2σ	$^{207}Pb/^{206}Pb$	± 2σ	
YAL-1																		
35170614b	35	378	177	280	0.47	20.3625	0.7598	0.6161	0.0223	0.2397	0.0076	3094	89	3109	36	3118	50	99
36170614b	36	264	96	187	0.36	19.6295	0.7301	0.6029	0.0218	0.2361	0.0074	3042	88	3073	36	3094	50	98
37170614b	37	350	232	249	0.66	18.2043	0.6782	0.5726	0.0207	0.2305	0.0073	2919	85	3001	36	3056	50	96
38170614b	38	226	31	148	0.14	19.1834	0.7170	0.5917	0.0214	0.2351	0.0075	2996	87	3051	36	3087	50	97
39170614b	39	105	25	57	0.24	13.4191	0.5074	0.4972	0.0180	0.1957	0.0063	2602	78	2710	36	2791	53	93
40170614b	40	500	229	331	0.46	17.4744	0.6513	0.5578	0.0202	0.2272	0.0072	2857	83	2961	36	3032	50	94
41170614b	41	256	78	180	0.31	19.9417	0.7452	0.6123	0.0221	0.2362	0.0075	3079	89	3089	36	3094	50	100
42170614b	42	107	28	57	0.26	13.0805	0.5138	0.4785	0.0176	0.1982	0.0068	2521	76	2686	37	2812	56	90
45170614b	45	90	24	53	0.27	14.5595	0.5544	0.5335	0.0194	0.1979	0.0065	2756	81	2787	36	2809	53	98
46170614b	46	136	37	71	0.27	12.5343	0.4743	0.4808	0.0174	0.1891	0.0061	2531	76	2645	36	2734	53	93
47170614b	47	203	90	144	0.44	19.6448	0.7410	0.5999	0.0217	0.2375	0.0076	3029	88	3074	36	3103	51	98
48170614b	48	406	140	272	0.34	18.4399	0.6938	0.5768	0.0209	0.2318	0.0074	2936	85	3013	36	3065	51	96
49170614b	49	156	80	110	0.51	18.9790	0.7206	0.5832	0.0212	0.2360	0.0077	2962	86	3041	37	3093	51	96
50170614b	50	82	80	57	0.98	14.7260	0.5625	0.5379	0.0196	0.1985	0.0065	2775	82	2798	36	2814	53	99
51170614b	51	191	103	137	0.54	19.2172	0.7282	0.5959	0.0216	0.2338	0.0076	3013	87	3053	37	3079	51	98
52170614b	52	104	41	56	0.40	12.9623	0.5168	0.4752	0.0175	0.1978	0.0069	2506	76	2677	38	2808	57	89
55170614b	55	356	201	264	0.57	19.9911	0.7585	0.6086	0.0221	0.2382	0.0077	3065	88	3091	37	3108	51	99
56170614b	56	214	42	133	0.20	17.9398	0.6864	0.5555	0.0202	0.2342	0.0077	2848	84	2987	37	3081	52	92
57170614b	57	158	64	107	0.40	18.8884	0.7299	0.5752	0.0210	0.2381	0.0079	2929	86	3036	37	3108	53	94
58170614b	58	277	136	175	0.49	16.7063	0.6421	0.5290	0.0193	0.2290	0.0076	2737	81	2918	37	3045	52	90
59170614b	59	148	51	100	0.34	18.0724	0.6950	0.5816	0.0212	0.2253	0.0074	2955	86	2994	37	3019	53	98
60170614b	60	113	49	70	0.44	14.7212	0.5760	0.5381	0.0197	0.1984	0.0067	2776	82	2797	37	2813	55	99

Table 3: Summary of the LA-ICP-MS results for the zircons analysed in this study.

Analysis	Grain Spot	U (ppm)	Th (ppm)	Pb (ppm)	Th/U	Isotopic ratios						Age Ma						Conc %
						$^{207}Pb/^{235}U$	± 2σ (abs)	$^{206}Pb/^{238}U$	± 2σ (abs)	$^{207}Pb/^{206}Pb$	± 2σ (abs)	$^{206}Pb/^{238}U$	± 2σ	$^{207}Pb/^{235}U$	± 2σ	$^{207}Pb/^{206}Pb$	± 2σ	
TON-1																		
07170614b	7	326	211	246	0.65	19.8696	0.7273	0.6106	0.0219	0.23597	0.0073	3073	88	3085	35	3093	49	99
08170614b	8	463	370	373	0.80	21.8213	0.7969	0.6328	0.0227	0.25007	0.0077	3161	90	3176	35	3185	49	99
09170614b	9	829	44	396	0.05	13.4509	0.4927	0.4418	0.0159	0.22077	0.0068	2359	71	2712	35	2986	50	79
12170614b	12	479	290	262	0.60	12.3854	0.4583	0.4512	0.0163	0.19907	0.0063	2400	72	2634	35	2819	51	85
15170614b	15	3334	400	1816	0.12	13.6721	0.4996	0.5079	0.0182	0.1952	0.006	2648	78	2727	35	2787	50	95
16170614b	16	2399	206	972	0.09	9.7081	0.3554	0.3844	0.0138	0.18312	0.0057	2097	64	2408	34	2681	51	78
17170614b	17	1035	477	686	0.46	18.0660	0.6611	0.5590	0.0201	0.23434	0.0073	2863	83	2993	35	3082	49	93
18170614b	18	721	619	587	0.86	21.1037	0.7733	0.6257	0.0225	0.24459	0.0076	3132	89	3143	36	3150	49	99
19170614b	19	424	263	280	0.62	15.0684	0.5540	0.5468	0.0197	0.19982	0.0062	2812	82	2820	35	2825	51	100
20170614b	20	397	148	289	0.37	20.8790	0.7684	0.6185	0.0223	0.24481	0.0076	3104	89	3133	36	3152	49	98
22170614b	22	700	537	553	0.77	20.6748	0.7606	0.6183	0.0223	0.24248	0.0076	3103	89	3124	36	3136	49	99
25170614b	25	1775	157	813	0.09	11.2054	0.4126	0.4352	0.0157	0.18671	0.0058	2329	70	2540	34	2713	51	86
28170614b	28	554	244	367	0.44	17.9088	0.6620	0.5531	0.0200	0.23479	0.0074	2838	83	2985	36	3085	50	92
29170614b	29	1364	1388	1025	1.02	18.2743	0.6739	0.5680	0.0205	0.23329	0.0073	2900	84	3004	35	3075	50	94
30170614b	30	423	133	262	0.31	14.8736	0.5500	0.5457	0.0197	0.19765	0.0062	2807	82	2807	35	2807	51	100
31170614b	31	166	67	102	0.41	14.3406	0.5351	0.5261	0.0190	0.19766	0.0063	2725	80	2773	35	2807	52	97

Table 3 : (Continued)

Analysis	Grain Spot	U (ppm)	Th (ppm)	Pb (ppm)	Th/U	Isotopic ratios						Age Ma						Conc (%)
						$^{207}Pb/^{235}U$	± 2σ (abs)	$^{206}Pb/^{238}U$	± 2σ (abs)	$^{207}Pb/^{206}Pb$	±2σ (abs)	$^{206}Pb/^{238}U$	± 2σ	$^{207}Pb/^{235}U$	± 2σ	$^{207}Pb/^{206}Pb$	± 2σ	
MANG-1																		
43270513	43	152	107	76	0.71	14.42489	0.3934	0.52967	0.013	0.19757	0.005	2740	56	2778	26	2806	40	98
44270513	44	1239	189	361	0.15	9.04033	0.2448	0.33754	0.008	0.1943	0.005	1875	41	2342	25	2779	39	67
45270513	45	27	18	14	0.64	14.33441	0.4101	0.53578	0.014	0.19409	0.005	2766	58	2772	27	2777	43	100
46270513	46	122	81	62	0.66	14.56689	0.4072	0.54246	0.014	0.19481	0.005	2794	58	2787	27	2783	42	100
47270513	47	153	100	78	0.66	14.70509	0.4047	0.54466	0.014	0.19586	0.005	2803	57	2796	26	2792	41	100
48270513	48	124	70	63	0.57	14.92693	0.4134	0.55019	0.014	0.19682	0.005	2826	58	2811	26	2800	41	101
49270513	49	64	55	34	0.85	15.06598	0.4252	0.53916	0.014	0.20272	0.005	2780	58	2819	27	2848	42	98
50270513	50	128	101	67	0.79	14.74365	0.4155	0.545	0.014	0.19626	0.005	2804	58	2799	27	2795	42	100
51270513	51	93	97	52	1.04	15.34103	0.4692	0.56011	0.015	0.1987	0.006	2867	63	2837	29	2816	48	102
52270513	52	280	121	136	0.43	14.55684	0.4024	0.5355	0.013	0.19721	0.005	2765	56	2787	26	2803	41	99
56270513	56	273	162	141	0.59	14.83312	0.4155	0.54959	0.014	0.1958	0.005	2824	57	2805	27	2792	42	101
57270513	57	20	12	10	0.59	14.88061	0.4387	0.54781	0.014	0.19707	0.006	2816	60	2808	28	2802	45	100
58270513	58	222	195	117	0.88	14.57528	0.4108	0.53121	0.013	0.19905	0.005	2747	56	2788	27	2818	42	97
59270513	59	225	72	106	0.32	14.40554	0.4073	0.53304	0.013	0.19606	0.005	2754	56	2777	27	2794	42	99
60270513	60	334	160	167	0.48	14.79171	0.4183	0.54871	0.014	0.19557	0.005	2820	57	2802	27	2790	42	101
61270513	61	108	77	57	0.71	14.95637	0.4288	0.54958	0.014	0.19743	0.005	2823	58	2813	27	2805	43	101
62270513	62	22	12	11	0.55	14.93738	0.4371	0.54819	0.014	0.19768	0.005	2818	59	2811	28	2807	45	100
63270513	63	63	68	35	1.07	14.35555	0.4143	0.54166	0.014	0.19227	0.005	2790	57	2774	27	2762	44	101
64270513	64	119	49	59	0.41	14.81777	0.4306	0.54275	0.014	0.19806	0.005	2795	58	2804	28	2810	44	99
65270513	65	112	71	59	0.63	14.98229	0.4317	0.55108	0.014	0.19724	0.005	2830	58	2814	27	2804	44	101
66270513	66	155	102	81	0.66	14.95356	0.4316	0.54881	0.014	0.19767	0.005	2820	58	2812	27	2807	44	100
67270513	67	76	56	40	0.73	14.57393	0.4258	0.54196	0.014	0.19509	0.005	2792	58	2788	28	2786	45	100
4270513	4	63	62	36	0.58	15.22572	0.4005	0.55899	0.014	0.19757	0.005	2863	57	2830	25	2806	38	101
5270513	5	18	11	10	0.91	15.05397	0.4099	0.55783	0.014	0.19575	0.004	2858	59	2819	26	2791	40	101
6270513	6	206	109	106	0.98	15.01524	0.3938	0.55764	0.014	0.19531	0.005	2857	57	2816	25	2787	38	101
7270513	7	182	105	95	0.91	15.15258	0.3991	0.56139	0.014	0.19578	0.006	2872	57	2825	25	2791	38	101

Table 3 : (Continued)

Analysis	Grain Spot	U (ppm)	Th (ppm)	Pb (ppm)	Th/U	Isotopic ratios						Age Ma						Conc (%)
						$^{207}Pb/^{235}U$	± 2σ (abs)	$^{206}Pb/^{238}U$	± 2σ (abs)	$^{207}Pb/^{206}Pb$	± 2σ (abs)	$^{206}Pb/^{238}U$	± 2σ	$^{207}Pb/^{235}U$	± 2 σ	$^{207}Pb/^{206}Pb$	± 2 σ	
LAG-1																		
11270513	11	161	44	75	0.27	14.6024	0.3796	0.5363	0.0134	0.1975	0.0044	2768.1000	56.380	2790	25	2806	36	99
12270513	12	128	42	60	0.33	14.4018	0.3758	0.5365	0.0135	0.1947	0.0044	2768.7000	56.500	2777	25	2783	37	100
13270513	13	78	84	42	1.08	14.4516	0.3784	0.5308	0.0134	0.1975	0.0045	2744.8000	56.220	2780	25	2806	37	98
17270513	17	62	65	34	1.05	14.6691	0.3935	0.5366	0.0137	0.1983	0.0047	2769.4000	57.460	2794	26	2812	39	98
18270513	18	59	70	39	1.19	20.8111	0.5522	0.6285	0.0160	0.2402	0.0056	3143.5000	63.160	3130	26	3122	37	101
19270513	19	74	90	42	1.21	15.0259	0.3984	0.5488	0.0139	0.1986	0.0046	2820.2000	57.740	2817	25	2815	38	100
20270513	20	125	114	68	0.91	15.1010	0.3994	0.5491	0.0138	0.1995	0.0046	2821.2000	57.640	2822	25	2822	38	100
21270513	21	133	93	69	0.70	14.4641	0.3853	0.5449	0.0138	0.1926	0.0045	2803.7000	57.560	2781	25	2764	38	101
22270513	22	178	122	88	0.69	13.7143	0.3622	0.4985	0.0125	0.1996	0.0046	2607.3000	53.940	2730	25	2823	37	92
23270513	23	212	158	103	0.74	13.7103	0.3597	0.4999	0.0125	0.1990	0.0045	2613.4000	53.740	2730	25	2818	37	93
24270513	24	144	34	66	0.24	14.3564	0.3771	0.5342	0.0134	0.1950	0.0045	2759.0000	56.140	2774	25	2785	37	99
25270513	25	81	82	44	1.01	14.6359	0.3967	0.5473	0.0140	0.1940	0.0047	2813.9000	58.240	2792	26	2776	39	101
26270513	26	138	129	71	0.94	14.1738	0.3844	0.5200	0.0133	0.1977	0.0048	2699.2000	56.340	2761	26	2808	39	96
30270513	30	110	114	65	1.04	16.0665	0.4277	0.5861	0.0147	0.1989	0.0047	2973.7000	59.800	2881	25	2817	38	106
31270513	31	92	60	47	0.66	14.7288	0.3931	0.5412	0.0136	0.1974	0.0047	2788.5000	56.880	2798	25	2805	38	99
32270513	32	185	173	99	0.93	14.8879	0.3980	0.5409	0.0136	0.1997	0.0047	2787.2000	56.860	2808	25	2824	38	99
33270513	33	86	88	46	1.02	14.2067	0.3837	0.5189	0.0131	0.1986	0.0048	2694.4000	55.680	2764	26	2815	39	96
34270513	34	367	28	145	0.08	12.1144	0.3223	0.4425	0.0111	0.1986	0.0047	2362.0000	49.400	2613	25	2815	38	84
35270513	35	136	37	63	0.27	14.2583	0.3811	0.5373	0.0134	0.1925	0.0046	2772.1000	56.380	2767	25	2764	39	100
36270513	36	46	39	25	0.85	15.1728	0.4192	0.5617	0.0144	0.1960	0.0049	2873.5000	59.380	2826	26	2793	41	103
37270513	37	85	61	45	0.72	14.9318	0.4062	0.5535	0.0140	0.1957	0.0048	2839.5000	58.080	2811	26	2791	40	102
38270513	38	138	43	65	0.31	14.6281	0.3946	0.5427	0.0136	0.1955	0.0047	2794.7000	56.940	2791	26	2789	39	100
39270513	39	83	52	43	0.63	14.7877	0.4011	0.5531	0.0139	0.1939	0.0047	2838.2000	57.780	2802	26	2776	40	102

Table 3 : (Continued)

Sample	Rock type	Crystallization age	Metamorphic age		Inheritance ($^{207}Pb/^{206}Pb$ age)
			Leonian	Liberian	
YAL-1	GGG	3098±19 Ma	3019±53 Ma	2812±14 Ma	
TON-1	GGG	3156±24 Ma	3093±49 Ma	2806±25 Ma	
MANG-1	Charnockite	2798±8 Ma			
LAG-1	Augen orthogneiss	2795±12 Ma			3121±37 Ma

Table 4: Summary of zircon U–Pb dating results obtained. GGG - Granulitic Grey Gneiss

Figure captions

Fig. 1: Geological sketch map of the West African Craton, adapted from Bessoles, 1977; Abouchami et al., 1990; Kouamelan et al., 1997; Egal et al., 2002; Persits et al., 2002; Peucat et al., 2005; Ennih and Liégeois, 2008; Pitra et al., 2010; Baratoux et al., 2011: Schofield et al., 2012. Redrawn after Berger et al., 2013.

Fig. 2: Schematic map of the Archean Man Domain in western Côte d'Ivoire with location of studied samples, adapted from Pitra et al., 2010.

Fig. 3: Concordia diagram for zircons from the YAL-1 granulitic grey gneiss sample analyzed with LA-ICP-MS, including transmitted light images of zircon grains with some ages obtained.

Fig. 4: Concordia diagram for zircons in the TON-1 granulite grey gneiss sample analyzed with LA-ICP-MS, including transmitted light images of zircon grains with some ages obtained.

Fig. 5 Concordia diagram for zircons in the Mangouion charnockite sample analyzed with LA-ICP-MS, including transmitted light images of zircon grains with some ages obtained.

Fig. 6: Concordia diagram for zircons in the Lagoulalé augen orthogneiss sample analyzed with LA-ICP-MS, including transmitted light images of zircon grains with some ages obtained.

.

I declare i have not any conflict of interest.

R.-Stéphane Gnagnon KOFFI

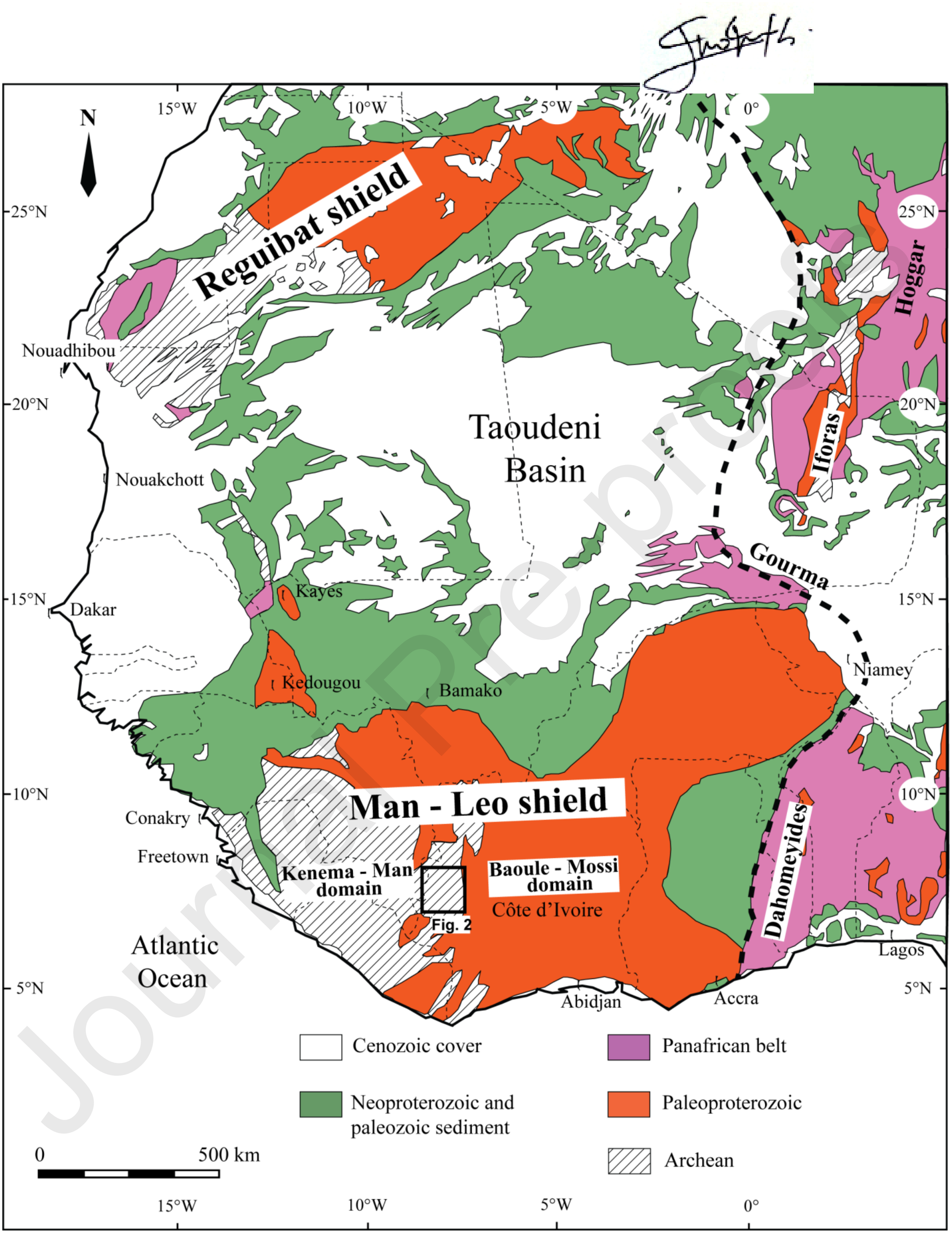

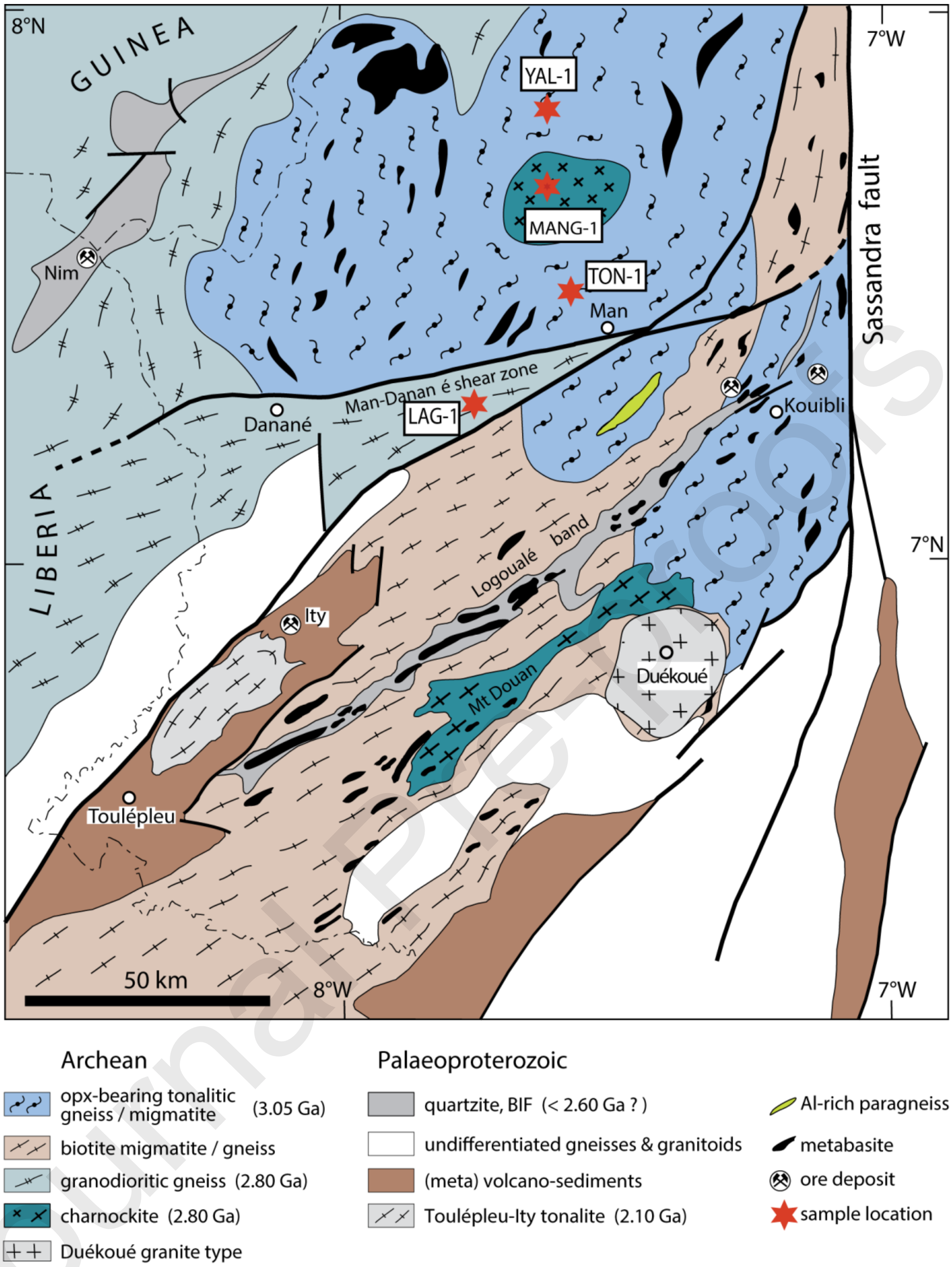

Fig. 2. Schematic map of the Archean part of the Man Rise (the Ke ́néma-Man domain) in western Ivory Coast and location of the studied sample DANT-1, MANg-1 et LAG-1 (star). Modified after Pitra et al., 2010.

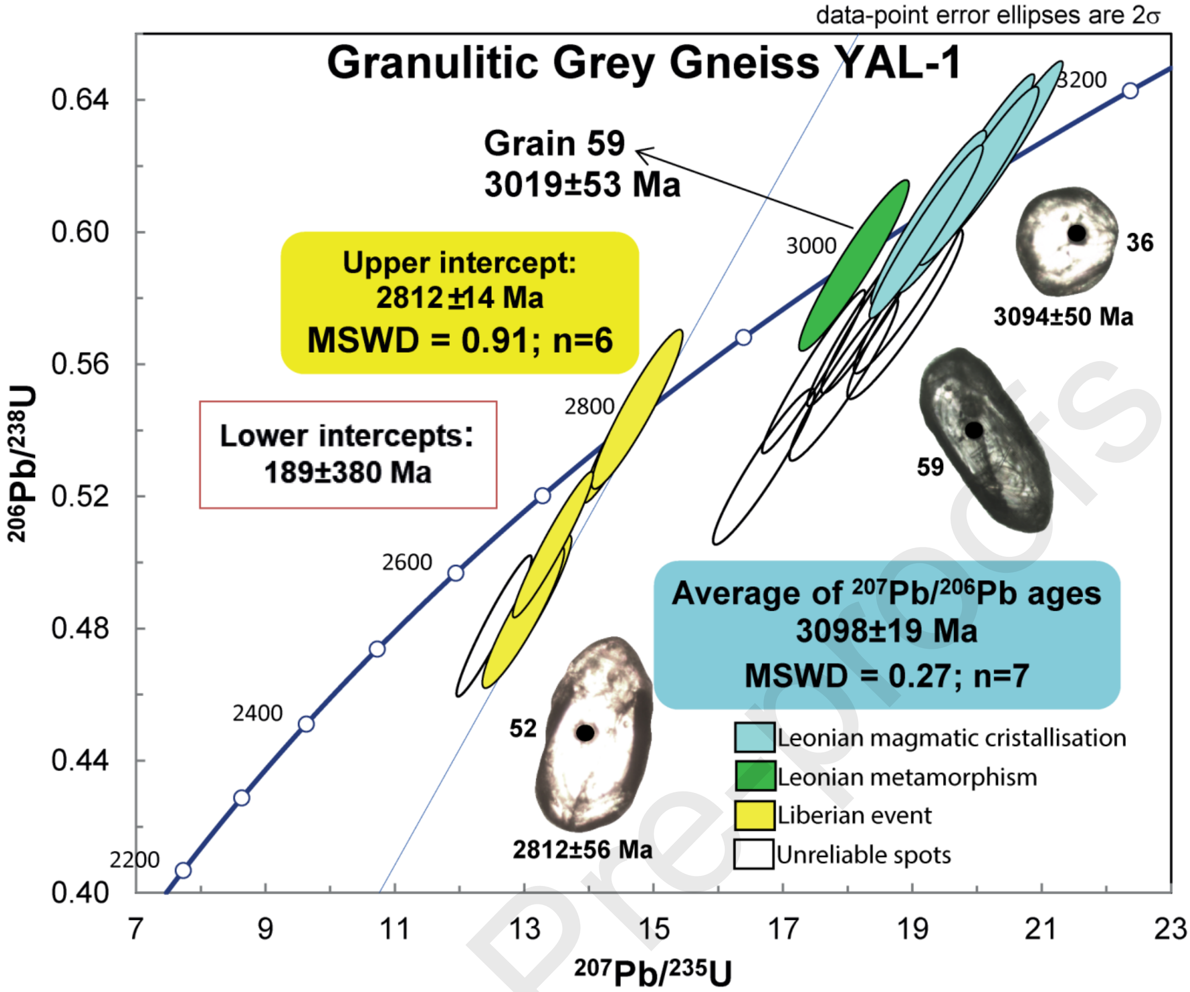

data-point error ellipses are 2σ
Granulitic Grey Gneiss YAL-1
Grain 59
3019±53 Ma
Upper intercept:
2812±14 Ma
MSWD = 0.91; n=6
Lower intercepts:
189±380 Ma
Average of 207Pb/206Pb ages
3098±19 Ma
MSWD = 0.27; n=7
36
3094±50 Ma
59
52
2812±56 Ma
Leonian magmatic cristallisation
Leonian metamorphism
Liberian event
Unreliable spots
3200
3000
2800
2600
2400
2200
0.64
0.60
0.56
0.52
0.48
0.44
0.40
7
9
11
13
15
17
19
21
23
206Pb/238U
207Pb/235U

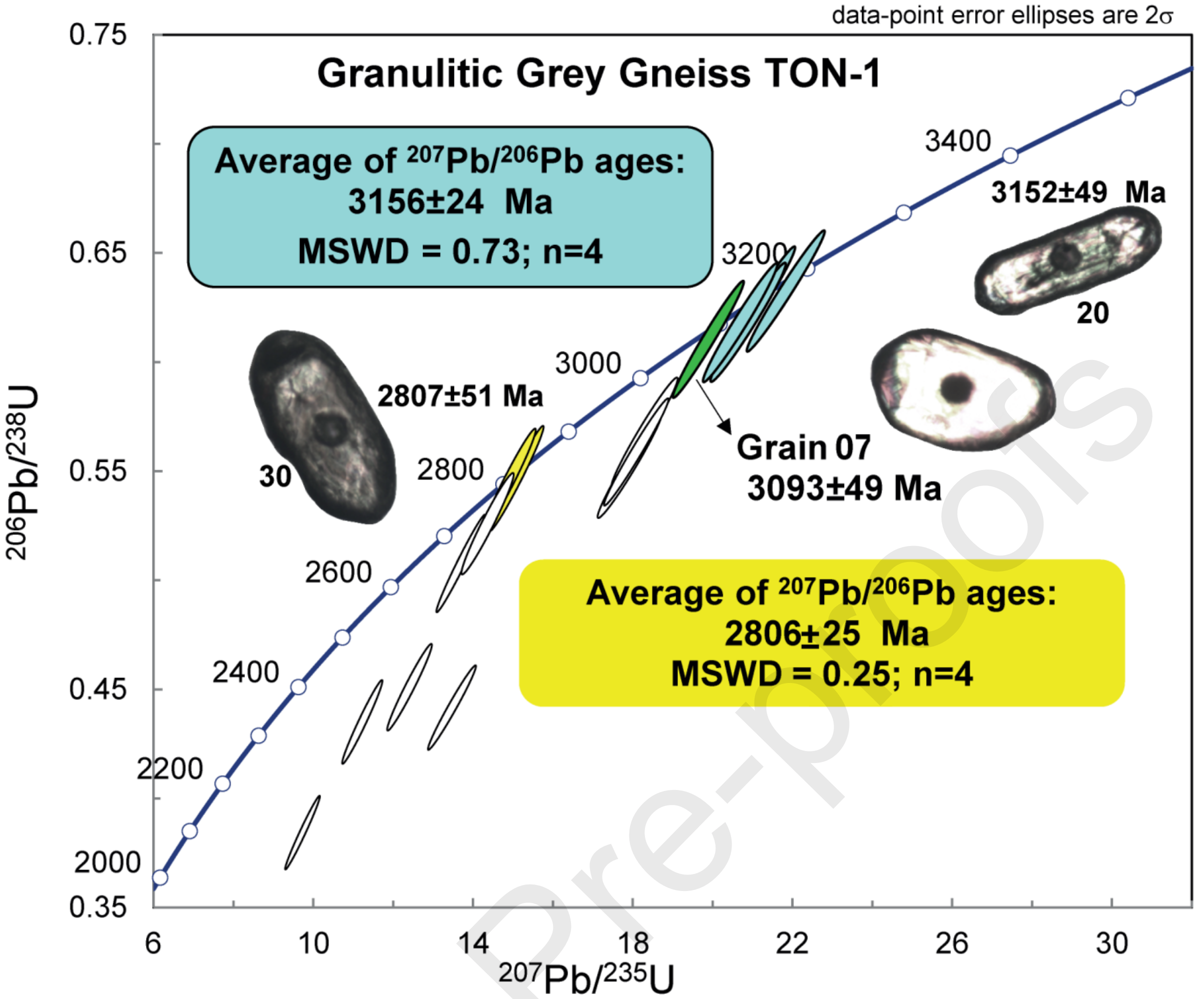
data-point error ellipses are 2σ
Granulitic Grey Gneiss TON-1
Average of 207Pb/206Pb ages:
3156±24 Ma
MSWD = 0.73; n=4
3152±49 Ma
20
2807±51 Ma
30
Grain 07
3093±49 Ma
Average of 207Pb/206Pb ages:
2806±25 Ma
MSWD = 0.25; n=4
0.75
0.65
0.55
0.45
0.35
206Pb/238U
207Pb/235U
6
10
14
18
22
26
30
2000
2200
2400
2600
2800
3000
3200
3400

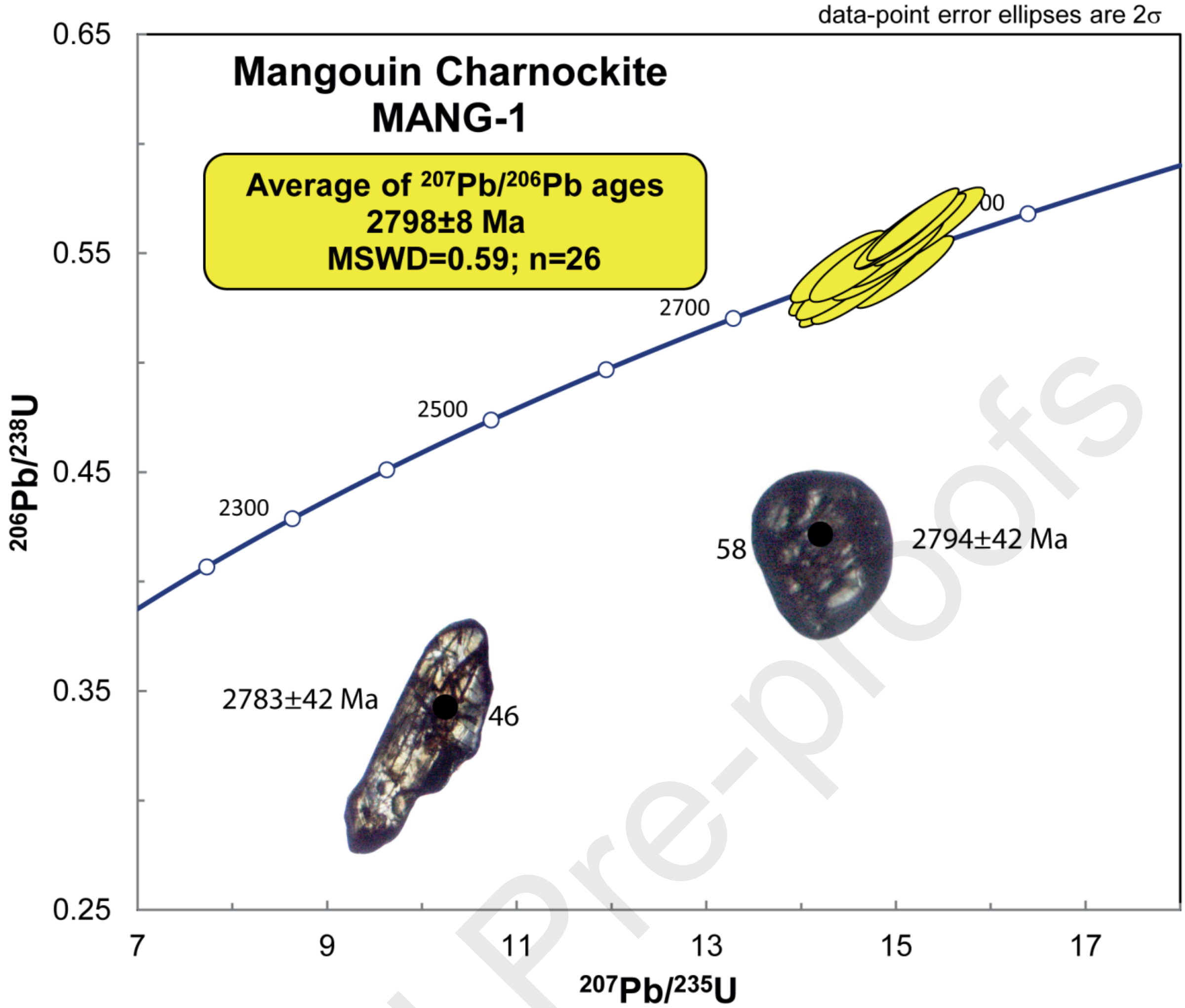
data-point error ellipses are 2σ
Mangouin Charnockite
MANG-1
Average of 207Pb/206Pb ages
2798±8 Ma
MSWD=0.59; n=26
2300
2500
2700
58
2794±42 Ma
2783±42 Ma
46
0.65
0.55
0.45
0.35
0.25
7
9
11
13
15
17
206Pb/238U
207Pb/235U

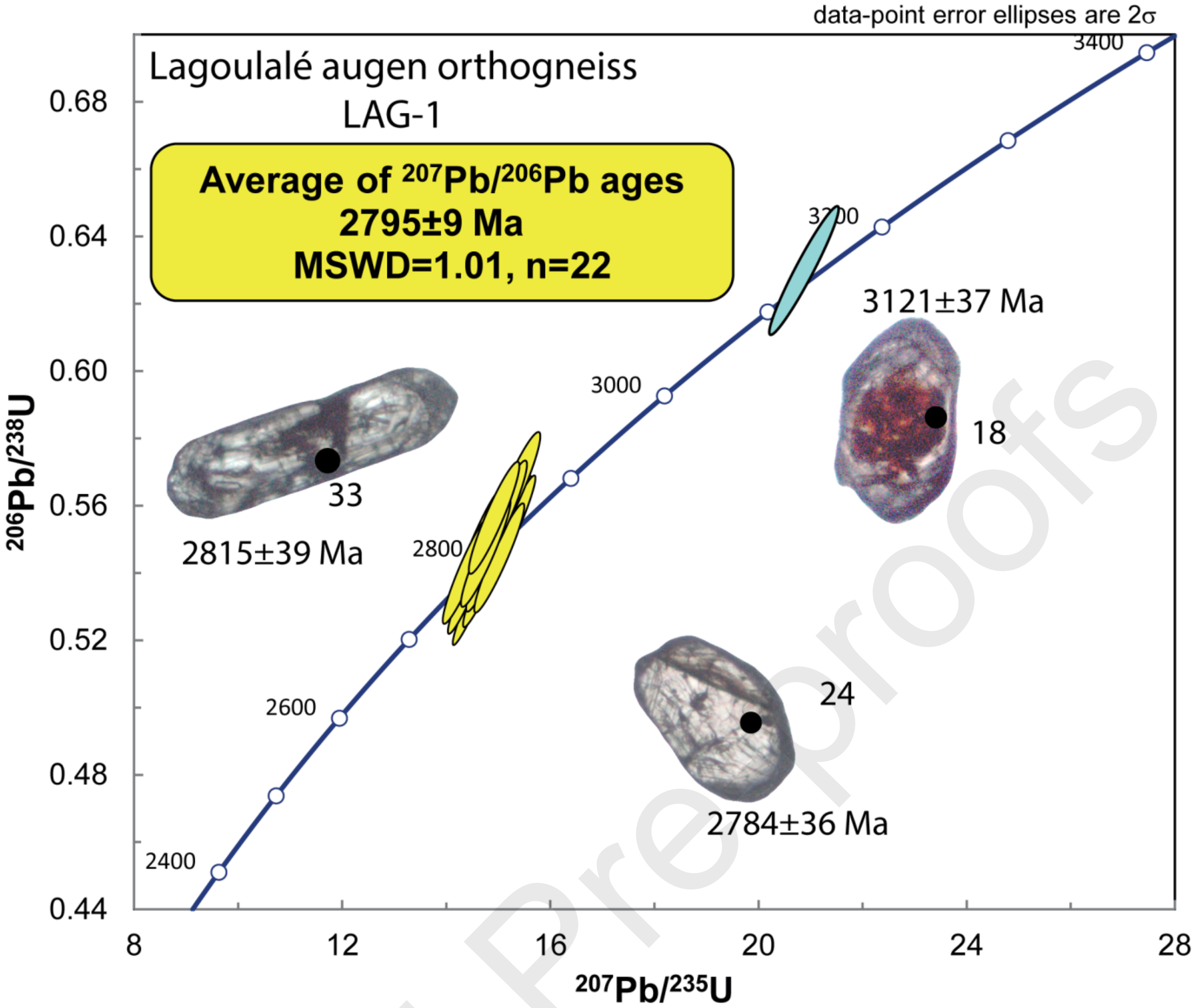
data-point error ellipses are 2σ
Lagoulalé augen orthogneiss
LAG-1
Average of 207Pb/206Pb ages
2795±9 Ma
MSWD=1.01, n=22
3121±37 Ma
18
33
2815±39 Ma
24
2784±36 Ma
2400
2600
2800
3000
3200
3400
0.68
0.64
0.60
0.56
0.52
0.48
0.44
8
12
16
20
24
28
206Pb/238U
207Pb/235U

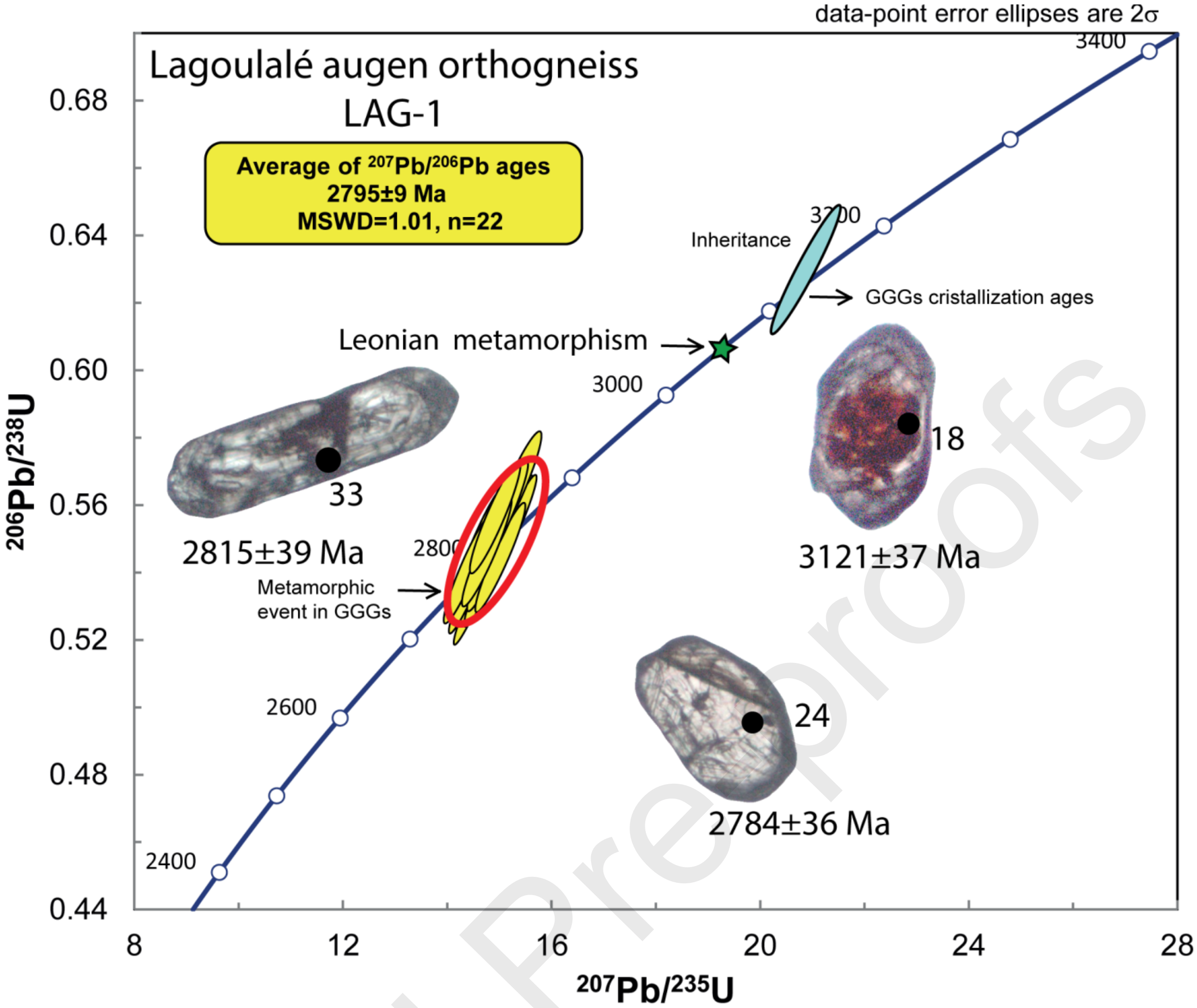

Highlights

- Leonian (3.3–3.0 Ga) and Liberian (2.9–2.7 Ga) are very distinct magmatic events.
- Leonian event has magmatism at 3.3–3.1 Ga followed by metamorphism at 3.1–3.0 Ga.
- Liberian magmatism corresponds to the reworking Leonian juvenile formations.